Environmental Modelling and Software 109 (2018) 17–31

Contents lists available at ScienceDirect

Environmental Modelling & Software

journal homepage: www.elsevier.com/locate/envsoft

Landscaping for road traffic noise abatement: Model validation

Timothy Van Renterghem*, Dick Botteldooren

Ghent University, Department of Information Technology, WAVES Research Group, Technologiepark 15, 9052, Gent-Zwijnaarde, Belgium

ARTICLE INFO

Keywords:
Outdoor sound propagation
Terrain effect
Engineering models
Full-wave models
Road traffic noise
Noise mapping

ABSTRACT

Deliberately changing terrain undulation and ground characteristics ("acoustical landscaping") is an potential noise abatement solution near roads. However, there is hardly any research regarding the validity of sound propagation models to predict its effectiveness. Long-term continuous sound pressure level measurements near a complex road traffic and sound propagation case were performed. Three types of modeling approaches were validated, covering the full spectrum of available techniques. A two-dimensional full-wave technique (the finite-difference time-domain method, FDTD), but also an advanced engineering model (the Harmonoise point-to-point model), provide accurate transmission loss predictions, both in 1/3 octave bands and for total A-weighted sound pressure levels. Two common and widely used semi-empirical engineering methods (ISO9613-2 and CNOSSOS) yield rather inaccurate results, notwithstanding the short propagation distance. The sensitivity to input data was assessed by modeling various scenarios with the FDTD method. Detailed ground effect modeling was shown to be of main importance.

1. Introduction

Road traffic noise has a serious impact on dwellers living near roads. This not only leads to a significant decrease in their quality of life (Botteldooren et al., 2011), but also to several proven health issues (for an overview, see Fritschi et al., 2011). In order to prevent excessive noise exposure, a combination of source measures, propagation measures and actions near the receiver can be taken. Although knowledge on these three groups of measures has increased over the last decades, noise exposure near roads is nowadays still a serious environmental threat. In the European Union, more than 100 million people are exposed to road traffic noise levels exceeding 55 dBA L_{den} inside the big agglomerations and along major road infrastructure (Nugent et al., 2014). This level is above the onset of negative health effects following the World Health Organization (Berglund et al., 1999).

This work deals specifically with actions to limit sound pressure levels from roads during propagation to the environment. The erection of a noise wall is a widely applied noise abatement solution (Kotzen and English, 2009). However, decades of practice have revealed some clear issues.

First, sound diffracts over the (top) edges of a noise wall. Although this leads to strong shielding at high sound frequencies, the low frequency part of the road spectrum is only affected to a limited extent. This causes a change in the spectral balance; the relatively increased low-frequency contribution is often held responsible for the rather low perceived efficiency ratings (Nilsson et al., 2008). In addition, their shielding strongly decreases with distance: a noise wall is only efficient in a relatively small zone behind it. This is not only inherent to the diffraction process, but is also caused by atmospheric effects. Even at close distance, the erection of such a non-streamlined object induces additional and strong (vertical) gradients in the horizontal component of the wind speed (e.g. De Jong and Stusnick, 1976; Salomons, 1999). This is detrimental for the (downwind) efficiency, even in the zone where - in absence of wind - reasonable shielding is expected. A third reason is that sound waves interact with natural (porous) soils, especially in case of a low height source like road traffic. The pronounced destructive interference this may cause is called the "ground dip". Its strength and spectral shape depends on the receiver height and distance relative to the source (Attenborough et al., 2007). This could lead to lower sound pressure levels in a significant part of the road traffic spectrum (Attenborough et al., 2007). In the presence of a screen, this ground effect is strongly reduced, limiting the overall insertion loss (relative to unscreened ground) (e.g. Jonasson, 1972; Embleton, 1996). Fourthly, audio-visual interactions were shown to be important for the perception of environmental noise barriers. Common non-natural and non-transparent noise walls typically perform badly in this respect (e.g. Maffei et al., 2013; Hong and Jeon, 2014). Finally, elongated noise walls negatively impact the social and ecological environment (Arenas, 2008).

The aforementioned issues with noise walls make landscaping an

* Corresponding author.
E-mail address: timothy.vanrenterghem@ugent.be (T. Van Renterghem).

https://doi.org/10.1016/j.envsoft.2018.08.012
Received 15 June 2018; Received in revised form 12 July 2018; Accepted 6 August 2018
Available online 09 August 2018
1364-8152/

attractive alternative noise abatement solution on condition there is sufficient space for its implementation. Acoustical landscaping is defined here as the optimization of the relief (shaping and ground cover) to increase the noise shielding of a source. Two common examples are depressing the road and raising the landscape near the road. Acoustical landscaping belongs to the group of so-called "environmental methods" (Nilsson et al., 2014) for the purpose of (surface transport) noise reduction. Some major noise-related advantages of acoustical landscaping should be stressed. A first one is the preservation of ground effects. Well designed earth mounds consisting of acoustically soft ground were measured and numerically predicted to provide at least the same amount of noise reduction as a noise wall of similar height (Busch et al., 2003; Arenas, 2008; Van Renterghem and Botteldooren, 2012). A second advantage is that a berm is less sensitive to refraction by wind. A non-steep and natural berm was predicted to outperform the shielding obtained by a noise wall in a long-term evaluation (Van Renterghem and Botteldooren, 2012). In addition, natural environments are highly preferred by people (Kaplan and Kaplan, 1989), leading to improved noise perception (for an overview, see Van Renterghem, 2018). Equivalent noise level reductions may exceed 10 dBA for noise annoyance when there is a view on vegetation (Van Renterghem, 2018). Finally, earth berms were shown to be most sustainable when compared to common steel or concrete roadside noise barriers (Oltean-Dumbrava and Miah, 2016). Life-cost analysis showed that berms are at least two times less expensive than common noise walls (Morgan et al., 2001), which is most likely a very conservative estimate when surplus ground is available at the project site.

However, predicting the impact of landscaping on sound propagation is not trivial. An ideal model should account for diffraction over arbitrary terrain, and at the same time, take into account the interactions between sound waves and natural grounds. In addition, such a computational technique should be sufficiently fast.

Full-wave numerical techniques are good candidates to model sound propagation in case of landscaping. Starting from the wave equations, diffraction, absorption and interferences are accurately accounted for. An interesting method is the finite-difference time-domain (FDTD) technique which will be used in the current work. This model has become a reference technique in outdoor sound propagation cases for wide-band environmental noise sources like road traffic (Van Renterghem, 2014).

However, two problems could appear with this type of highly detailed models. A first practical issue is getting sufficiently detailed input data. The spatial resolution used in such models is typically at the centimeter scale, which is needed to sufficiently discretise the wavelengths of interest. Clearly, such data will not be commonly available. Some care is needed since input data simplifications could give rise to some "artifacts". A known example is the prediction of too strong (destructive) interferences by assuming ground (slope) simplifications. Although physically correct, this will not appear in practice due to small variations in terrain undulation and ground impedances that are always present, or even by a small degree of atmospheric scattering. A question remains to what extent e.g. geometrical data needs to be taken into account for accurate predictions of sound exposure levels near roads. A second issue is the strong need for computational resources. As a result, calculations are most often performed in two dimensions or by limiting the maximum sound frequency that is resolved. One could potentially question to what extent such a simplification would cancel the accuracy gained at other instances during the modeling process.

At the other end of the modeling spectrum, so-called engineering methods appear. They try to approach the complex sound propagation physics by a set of simplified (and semi-empirical) formulae that allow an easy - and especially – a fast evaluation. A widely used technique in noise mapping is ISO9613-2 (ISO 9613-2, 1996). The method is expected to predict long-term averaged sound pressure levels with an accuracy of 3 dBA for low-height (broadband) sound sources (source height below 5 m) within 100 m distance from the source (ISO 9613-2, 1996). The accuracy in case of terrain undulations was not reported and has not been put to the test before. The more recently developed CNOSSOS (Kephalopoulos et al., 2012) propagation module is considered here as well. This method is the advised engineering method for future strategic noise mapping in the framework of the European Commission's Environmental Noise Directive issued in 2002. The method itself is largely inspired by the French national method for sound propagation near roads (Dutilleux et al., 2010), and has a slightly higher model complexity than the ISO9613-2 model. Quantification of their accuracy is needed since such methods are most often used for making noise maps (Licitra, 2013; Keyel et al., 2017).

In between these two extremes, the Harmonoise point-to-point propagation (HP2P) module (Van Maercke and Defrance, 2007) balances between physical accurateness but still allowing a reasonably fast evaluation. Arbitrary terrain undulations can be taken into account. HP2P was shown to yield accurate long-term averaged predictions near a highway in a flat environment and in the case of an embankment. Comparisons with other numerical (reference) models, but also with measurements, lead to deviations below 1–1.5 dBA (at distances smaller than roughly 1 km) (Defrance et al., 2007). The spectral accuracy, and the accuracy at receiver heights below 4 m, have not been reported, nevertheless. Such a validation is however most challenging.

In this study, the above-described modeling approaches will be validated in a complex road traffic noise case, including terrain undulations. Not only detailed long-term noise measurements are available, but also on-site traffic counts and terrain elevation data at a fine spatial resolution. Although there are many other propagation methods, mostly national ones, the engineering techniques considered here (ISO9613-2, CNOSSOS and HP2P) were developed on an international plan, are widely used, and fully cover the range in complexity one can find.

2. Site description

The case of interest is a segment of the Antwerp ring road, bordered by a cycling path on top of a 6.3-m high embankment (relative to the road surface). The current case could also be considered as a depressed road. At this location (see Figs. 1–3), the highway consists of 8 lanes with a high share of heavy vehicles. There are 5 lanes closest to the microphone positions, and 3 lanes in the opposite driving direction. The far lanes are partly shielded by a double row of 0.7-m high concrete jerseys. In between these jerseys, some very sparse vegetation and a layer of top soil was present, constituting the middle verge. At about 240 m (in southwestern direction, measured along the highway) and 320 m (in northeastern direction, measured along the highway) from the cross-section under study two bridges cross the highway. The stretch of highway between these bridges has a length of 560 m and can be considered as the dominant sound contribution in this cross section.

A first measurement position (MP1) is located directly bordering the highway, a about 30 m from the centre of the middle verge. Measurement point 2 (MP2) is located on top of the embankment, at about 80 m from the centre of the middle verge. The microphone heights were at both positions 1.75 m above the ground. Near its top, a zone of 20 m of tall (but sparse) trees is present. A detailed assessment of the vegetation belt was not made. In front of MP2, there is a 3-m wide cycling path.

3. Measurement campaign

3.1. Meteorological data

Basic meteorological data was available from a (standard) meteorological measurement station at roughly 15 km from the site under study. The data (see Fig. 4) was primarily used to remove rainy and windy periods to ensure adequately measured sound pressure levels. Secondly, air temperature, relative humidity and atmospheric pressure

Fig. 1. Overall impression of part of the highway under study, with indication of the microphone positions. The traffic counting stations are visible at close distance in southwestern direction relative to MP1.

were used to estimate the amount of atmospheric absorption. Averaged values during the day time (7:00 h–22:59 h) period were 15.2 °C, 73.7% and 101480 Pa; during the night period (23:00h-6:59 h) 11.9 °C, 84.9% and 101440 Pa, respectively. Most of the time, the wind was blowing mildly from south-western direction.

3.2. Sound pressure level measurements

Continuous sound pressure level measurements ($L_{eq,200\,ms}$, in 1/3 octave bands) were conducted during almost a full month to characterize in detail the sound propagation between the close point (MP1), directly bordering the highway, and the second one on top of the embankment (MP2).

Two independent type-1 accredited measurement chains were used, consisting of battery driven SVAN959 (Svantek) sonometers, with SV12L (Svantek) preamplifiers and ½" BK 4189 (Bruel & Kjaer) microphone capsules. Weather proof outdoor units (WME 950, Microtech Gefell) with birdspikes were used. At the start of the experiment, an (in-situ) calibration was performed with a type-1 SVAN30A pistonphone (Svantek) emitting a single sound frequency of 1 kHz at 114 dB. The calibrations were checked weekly and deviations ranged between −0.1 and 0.1 dB. The clocks of the sonometers were manually synchronized (expected accuracy of 1 s) at the beginning of the measurement campaign. To account for desynchronisation of the clocks over time, equivalent sound pressure levels were further integrated to 5-min intervals.

The sound pressure levels over the full measurement period are depicted in Fig. 5. At MP2, there were a few days of missing data due to microphone failure. Near the moments of calibration checks, data from half an hour before and half an hour after this operation were removed to prevent influencing the measurements (operator approaching the microphone, opening the fence at MP2 – see Fig. 3, etc.). In addition,

Fig. 2. A more detailed orthophoto of the microphone positions, with indication of the traffic lane numbering.

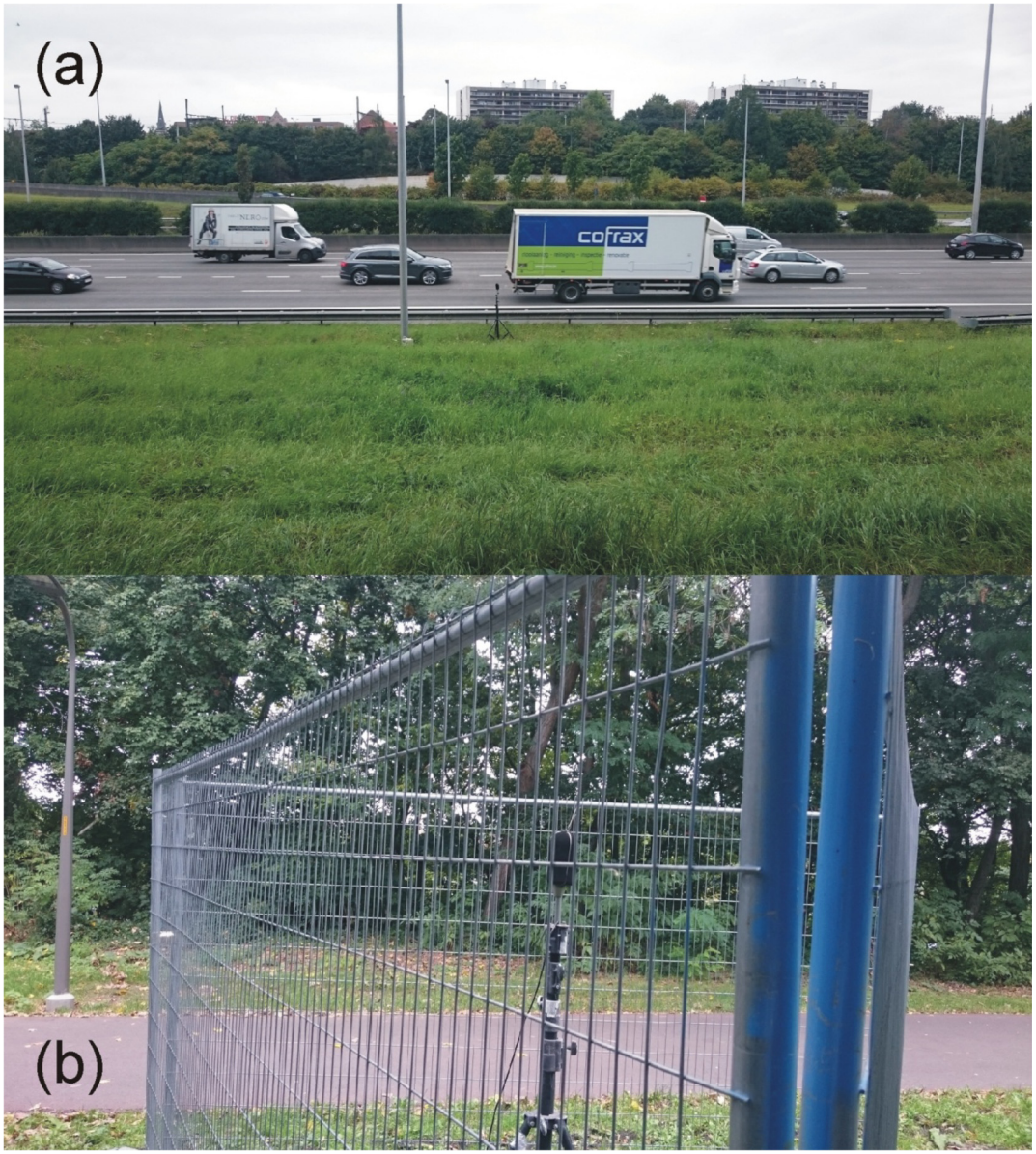

Fig. 3. Photographs of the microphones MP1 (a) and MP2 (b) taken towards the highway.

measurements from the meteorological post were used to remove periods with (any) rain and wind speeds (measured at 10 m height) exceeding 5 m/s.

Fig. 5 shows the typical day-night pattern, with local maxima typically near morning and evening rush hours. During daytime, a rather constant level is reached, with accidental decreases due to traffic jams. At night, at about 3 a.m., minima appear. At MP1, the median $L_{eq,5min}$ equals 83.5 dBA (with the statistical levels $L_{5,5min}$ = 85.8 dBA and $L_{95,5min}$ = 78.1 dBA). At MP2, the median $L_{eq,5min}$ is 69.3 dBA (with $L_{5,5min}$ = 71.6 and $L_{95,5min}$ = 63.8 dBA). At MP1, the highway is by far the dominant contribution since its placement directly near the road (see Figs. 1 and 2). At MP2, a close resemblance (see Fig. 5) is observed with the time evolution at MP1, indicating that highway noise is dominant there as well.

The boxplots in Fig. 6 show that the measured spectral level differences are quite consistent over this period; the interquartile distances stay roughly between 2 dB for all 1/3 octave bands. This small variation could find its origin in changes in lane use over time, ground impedance variations at the embankment due to changing soil water content (e.g. Cramond and Don, 1987; Guillaume et al., 2015) and meteorological effects (like short-distance refraction or changing atmospheric absorption). At the higher sound frequencies (above 5 kHz), the variation in level difference over time is somewhat more enhanced. Above 10 kHz (not shown), this level difference tends to zero due to insufficient signal-to-noise ratio; the road traffic does not produce a significant amount of energy in that frequency range (Sandberg and Ejsmont, 2002).

The increase in spectral level difference between MP1 and MP2, centered around 400–500 Hz, nicely illustrates a main advantage of a (natural) berm: the ground effect is preserved to a substantial extent. Behind a noise wall, in contrast, this (soft) ground effect would have been lost. Note that this noise abatement comes on top of the terrain shielding which generally increases with sound frequency.

The total A-weighted level difference statistics over the full month are shown in Fig. 7. The interquartile distance is limited to 1.5 dBA. The median difference is 14.2 dBA.

To conclude, the measurements show sufficiently complex sound propagation effects involving a combination of terrain shielding and a pronounced ground effect. Although outliers are inevitable in such unsupervised measurements, the bulk of the level differences, even per

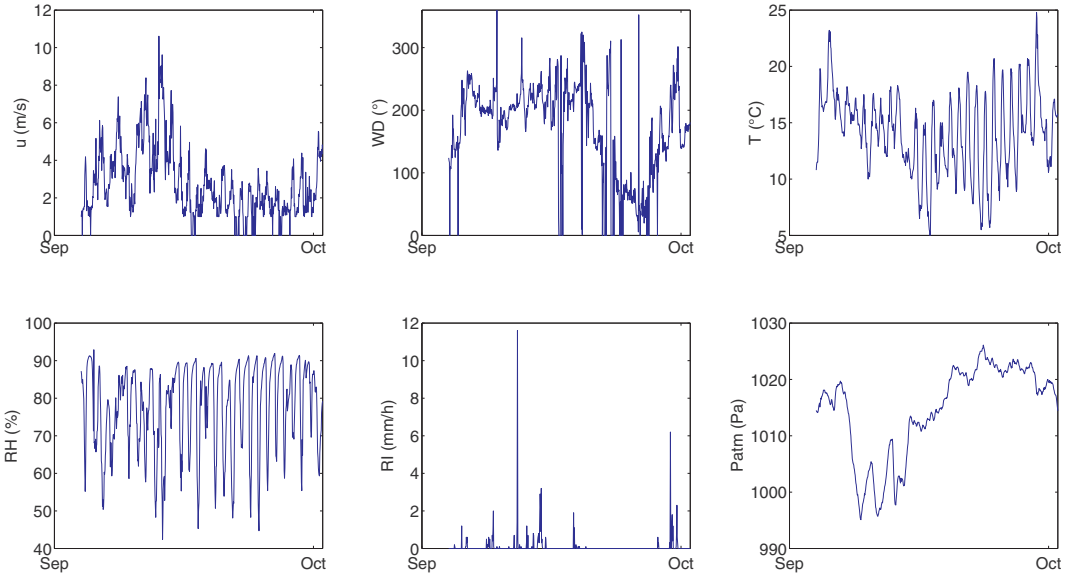

Fig. 4. Meteorological observations near the measurement site (with *u* wind speed, *WD* wind direction where 0° indicates northern wind, *T* air temperature, *RH* relative humidity, *RI* rainfall intensity and *Patm* atmospheric pressure) on an hourly basis.

1/3-octave band, are quite constant over this rather long measurement campaign. In addition, highway noise is clearly the dominant contribution to the sound field at both measurement points. This case thus provides an interesting validation opportunity for sound propagation models.

4. Input data and sound propagation modeling

The validation exercise conducted here focuses on sound propagation models, and not on road traffic source power models. However, the flow balance between the different lanes is relevant when modeling the (combined) exposure at the measurement points. The multi-lane road traffic case studied here is quite complex. The sound from some lanes could reach MP1 and/or MP2 by line-of-sight propagation, while other contributions become shielded by either the central verge or the embankment. The Harmonoise/Imagine source power model (Jonasson, 2007) has been used for all prediction methods considered. This is not only for reasons of consistency, but also because this model provides predictions at the detail of 1/3 octave bands. Using a single source power model allows a fairer comparison since the focus here is on the propagation modules.

4.1. Traffic data and source power levels

Detailed traffic data is available on a 1-min basis. The original data distinguishes between 4 vehicle categories, which have been reduced to 3 categories (light *LV*, medium-heavy *MHV* and heavy vehicles *HV*) to be consistent with the Harmonoise/Imagine source power model (Jonasson, 2007). Vehicle speed, per category, and intensity, per category, are available for each of the 9 lanes present near the counting station. Once passed this counting station (see Fig. 1), the two closest lanes to the microphones merge (and become lane number 8, see Fig. 2).

The zone under study is characterized by intense traffic, and contains a high share of (medium) heavy vehicles. In the SW direction, the daily averaged (during the month under study) traffic intensity (over

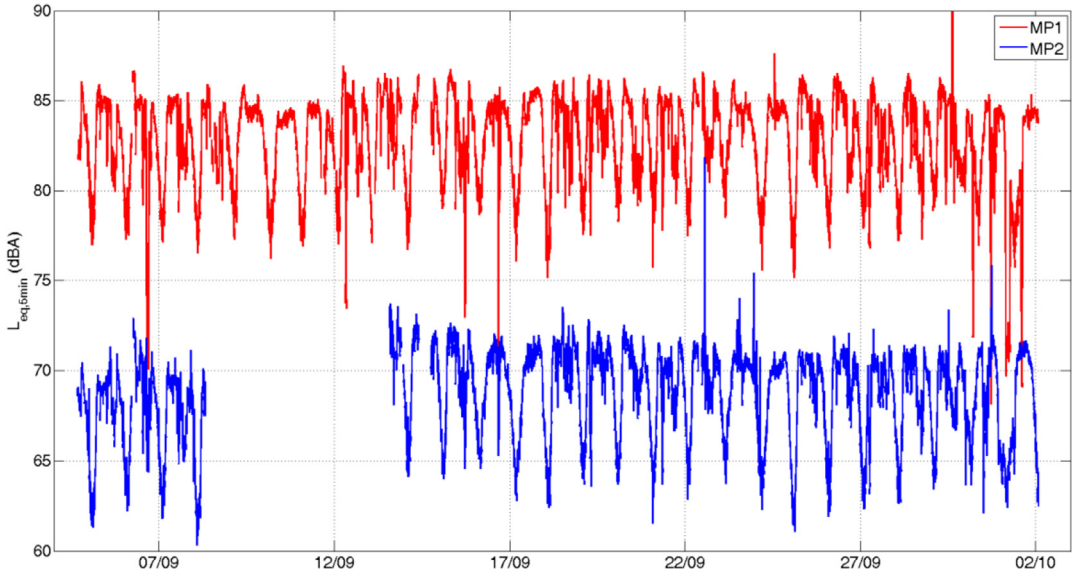

Fig. 5. Measured sound pressure levels at the microphone positions during the measurement campaign.

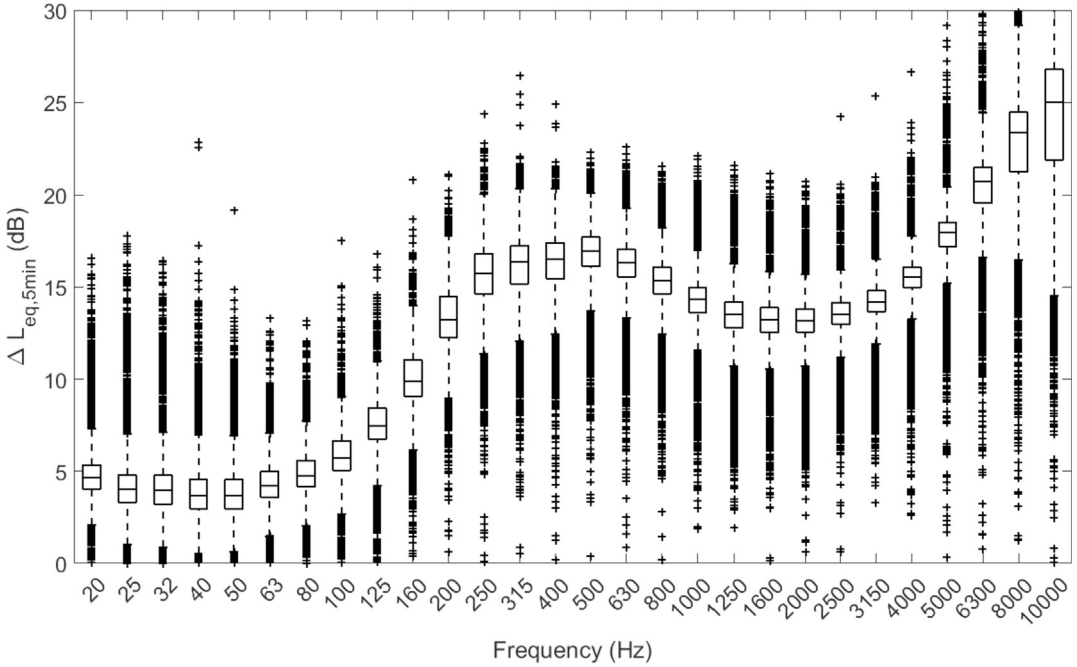

Fig. 6. Boxplots showing the spectral level differences $\Delta L_{eq,5min}$ between MP1 and MP2. The (middle) horizontal line in each box indicates the median of the data. The boxes are closed by the first and third quartile. The whiskers extend to 1.5 times the interquartile distance above the maximum value inside each box, and to 1.5 times the interquartile distance below the minimum value inside each box. Data points that fall outside these limits (outliers) are indicated with the plus-signs.

24 h) is 72 100 (sum of lanes 1 to 3, with 60% LV, 26% MHV and 14% HV), in the NE direction 136600 vehicles (sum of lanes 4 to 8, with 68% LV, 18% MHV and 14% HV). The zone under study is sensitive to congestion, leading to an average vehicle speed (over all lanes, all vehicle types) of 87 km/h.

In Figs. 8 and 9, the relative source powers per lane are shown during the day (a) and night hours (b). The average vehicle speed and total intensity per period, per lane and per vehicle category were used to compile this figure. The sound production by the highway during day time and night time is quite different. At night, there is a smaller share of heavy traffic relative to light traffic, and there are higher vehicle speeds due to the lower traffic intensity. Consequently, this leads to the relatively larger contribution of rolling noise frequencies at night. During daytime, the highest (averaged) driving speeds are found at lanes 3 to 5, leading to a more intense high frequency sound radiation relative to the other lanes. At night, lanes 1 and 6 are most frequently used, while lanes 3 and 4 (these are the fast lanes for traffic in the SW and NE direction, respectively) are less used.

4.2. Ground elevation data

Terrain elevation data is available as a non-uniform point scatter. In Fig. 10, an interpolation to a uniformly spaced map is presented. The depressed road and embankment are clearly visible. The somewhat raised middle verge can be observed as well.

In case of the FDTD model, used in two-dimensions here, the closest cross-section near the measurement points was used, approached by staircase fitting (however, with a very small spatial resolution of 0.02 m, see further). For the HP2P model, the terrain cross section is approached by linear segments, using the so-called iterative end-point fit algorithm to minimize the number of segments (Ramer, 1972), with a maximum deviation relative to the actual profile set at 0.1 m. In

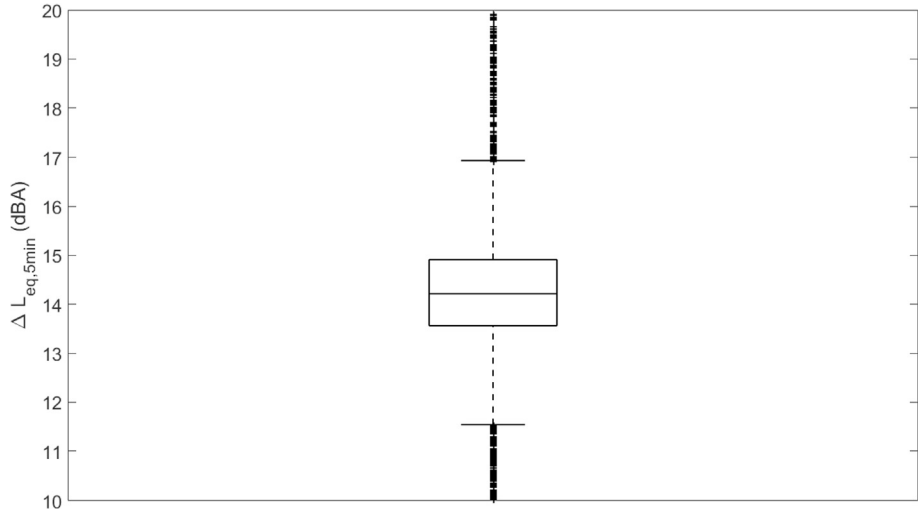

Fig. 7. Boxplot showing the total A-weighted level difference $\Delta L_{eq,5min}$ between MP1 and MP2.

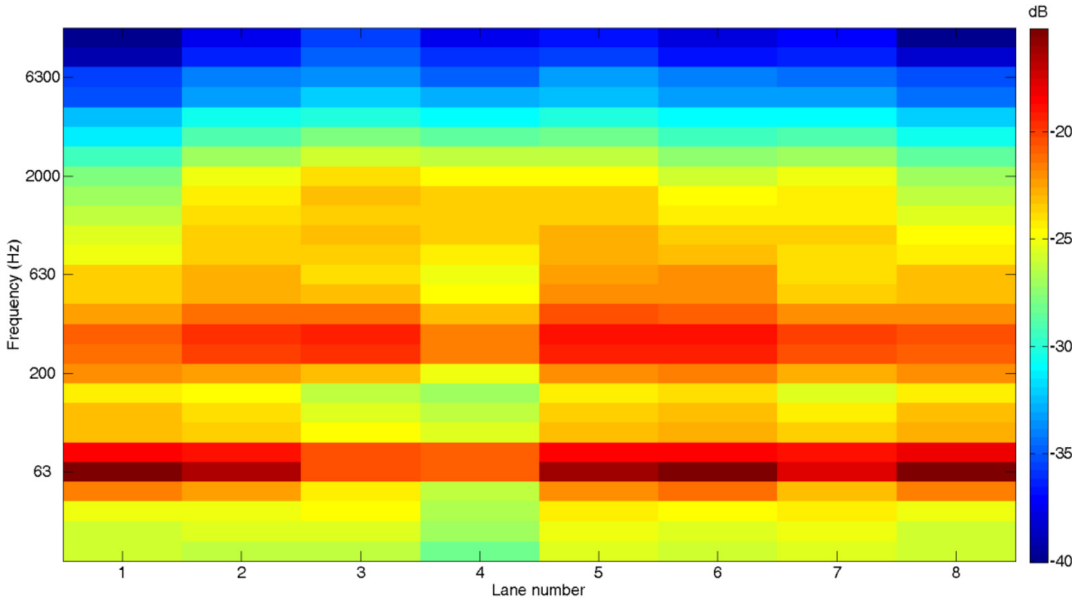

Fig. 8. Relative source power level per lane during the day hours (7:00h-22:59 h), when using the Harmonoise/Imagine source power model, using on-site traffic data during the measurement campaign. The energetic sum from all lanes and all 1/3-octave bands equals 0 dB [color online].

ISO9613-2 and CNOSSOS, the elevation data in this cross-section is approached by the best fitted line on the profile between each source-receiver combination. These profile approaches are illustrated in Fig. 11.

4.3. Ground characteristics

Ground property data is derived from a site visit and from visual inspection of orthophotos. Near the border of the road, the embankment consists of rather rough grassland with tall grass. Near the top of the embankment, a zone with a vegetation soil (similar to a forest floor) is present consisting of plant litter and a well-developed humus layer. The surface of the cycling path is dense and smooth asphalt. On top of the embankment, zones of maintained grassland are present. The highway itself has a concrete surface layer.

4.4. Sound propagation modeling

4.4.1. Finite-difference time-domain (FDTD) method

Sound propagation in a non-moving and homogeneous medium is described by following linear equations (Van Renterghem, 2014):

$$\nabla \cdot p + \rho_0 \frac{\partial \boldsymbol{v}}{\partial t} = \mathbf{0} \tag{1}$$

$$\frac{\partial p}{\partial t} + \rho_0 c_0 \nabla \cdot \boldsymbol{v} = 0 \tag{2}$$

In these equations, p is the acoustic pressure, v is the particle velocity, ρ_0 is the mass density of air, c_0 is the adiabatic sound speed, and t denotes time. Viscosity, thermal conductivity, and molecular relaxation are (initially) neglected.

The 2D staggered-in-time and staggered-in-space numerical approach has been used to discretise these equations, using a structured

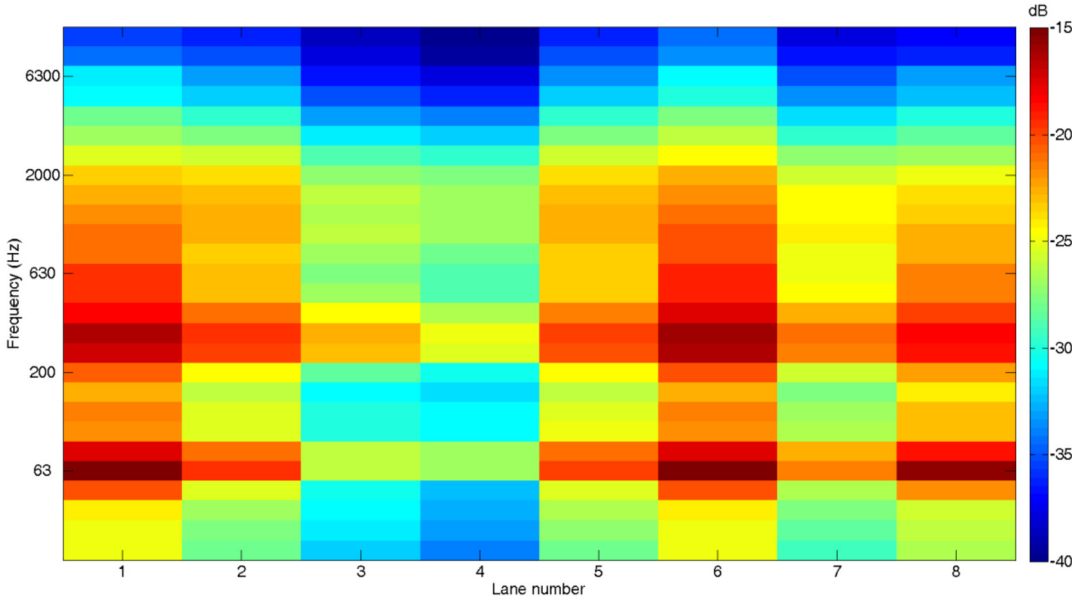

Fig. 9. See caption of Fig. 8, but now for the night hours (23:00h-6:59 h).

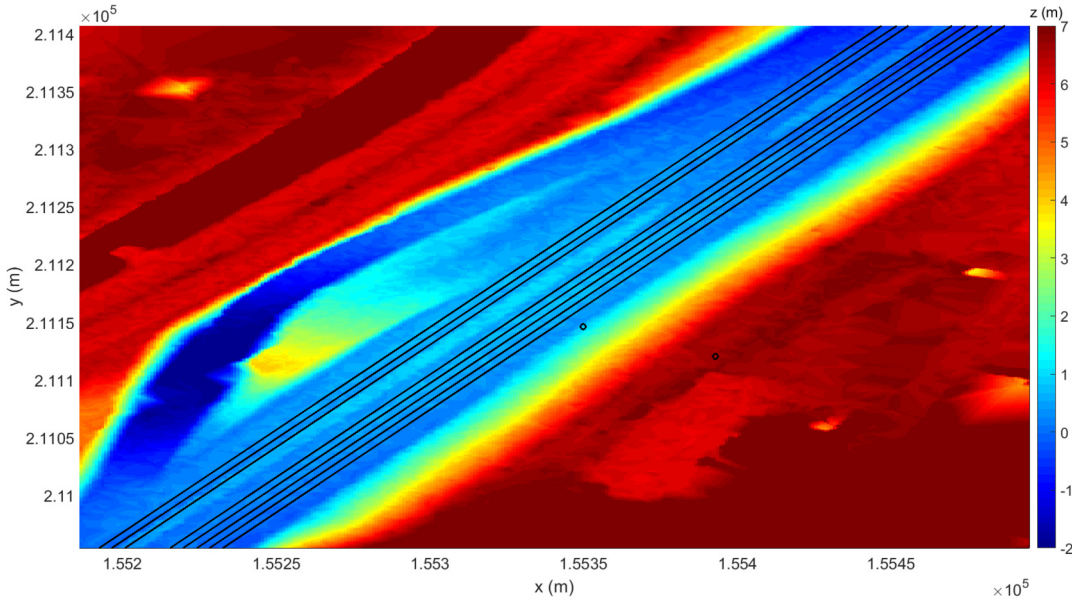

Fig. 10. Digital elevation map (in Lambert-72 geographical coordinates), with indication of the highway traffic lane centers (black lines) and the measurement points (the two open black circles).

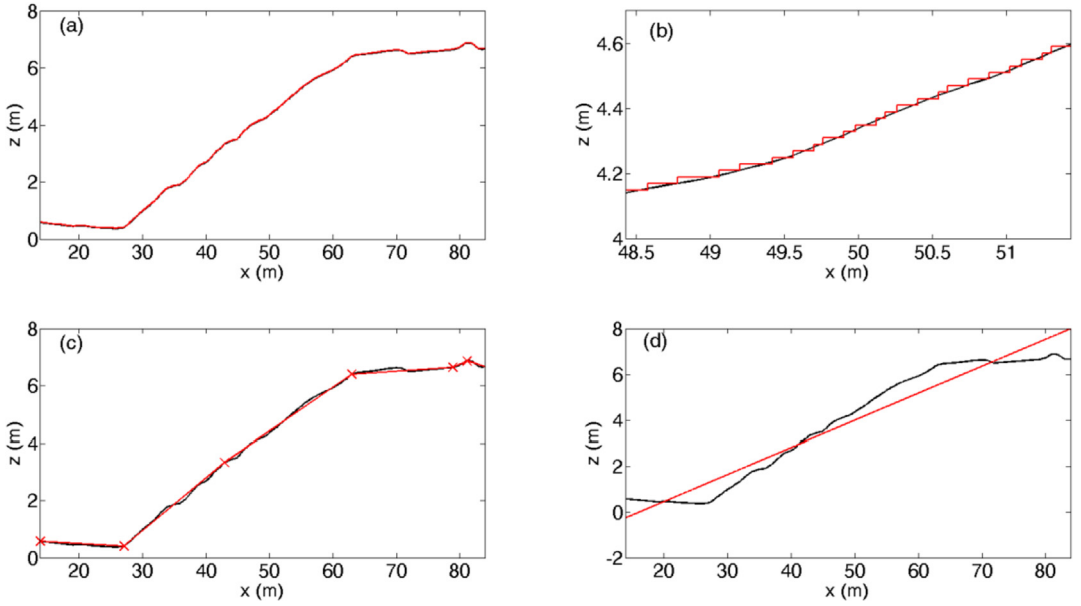

Fig. 11. Approaching the slope in the current case study with the FDTD method [(a) and (b), the latter being a zoom-in], with the HP2P model (c), and with ISO9613-2 and CNOSSOS (d). The black line is the actual profile, the red lines are the profiles used in the models (not true to scale).

Cartesian computational grid built-up by both acoustic pressures and particle velocity components. See Van Renterghem (2014) for a detailed discussion of the advantages of these specific discretisation choices. A pulse-like source excitation is used to estimate sound transmission over a wide range of frequencies with a single simulation (and applying a Fourier transform afterwards). This is an efficient approach since road traffic noise has a rather broad frequency spectrum. Since this is a generic source excitation ("pressure injection"), a frequency dependent correction is made to account for the actual road traffic source power spectrum considered for each 1/3 octave band (see Section 4.1).

A small layer of ground medium (0.5-m deep) is included in the simulation domain itself, accounting for non-locally reacting sound-soil interactions (see e.g. Attenborough et al., 2007). The Zwikker and Kosten phenomenological (ground) model (Zwikker and Kosten, 1949) has been used, which allows an efficient implementation in the FDTD context (Van Renterghem, 2014). Averaged parameters for grassland and forest floor, as found in Attenborough et al. (2011), have been used. Note that these ground parameters (see Table 1) are the result of fitting on large sets of measurements, specifically for the implemented model.

For each lane, a separate sound propagation simulation was made. To ensure full incoherence between the different lanes, their contributions are energetically summed at a receiver. Nevertheless, the two dimensional simulations performed here imply that each separate traffic lane is approached as a coherent line source. This – at least in theory – conflicts with the fact that vehicles on a road emit sound independently from each other. Adding multiple lanes incoherently will reduce the coherence generated by a single lane.

Atmospheric absorption has been included afterwards using ISO9613-1 (ISO 9613-1, 1996), based on the line-of-sight distance between each source and receiver point. Although this effect could have

Table 1
Overview of the computational parameters used in the finite-difference time-domain (FDTD) model.

Model parameter	Value
Spatial discretisation step (square cells)	0.02 m
Temporal discretisation step	40 μs
Speed of sound	340 m/s
Mass density of air	1.2 kg/m^3
Number of time steps	17500
Maximum sound frequency considered	upper frequency of the 1/3 octave band with centre frequency 1.6 kHz
Perfectly matched layer (PML) thickness	40 cells, with (numerically) optimized damping parameters.
Ground layer thickness	0.5 m deep, rigid backing.
Ground parameters forest floor	"Effective" flow resistivity = 20 kPas/m^2, "effective" porosity = 0.50 (Zwikker and Kosten model) (Zwikker and Kosten, 1949).
Ground parameters grassland	"Effective" flow resistivity = 300 kPas/m^2, "effective" porosity = 0.75 (Zwikker and Kosten model) (Zwikker and Kosten, 1949).
Building outer surface impedance (brickwork)	$37Z_0$, with Z_0 impedance of air (frequency independent real impedance), equivalent to an absorption coefficient at normal incidence α_0 of 0.1 (Cox and D'Antonio, 2004).
Vegetation scattering	Single computational cells (4 cm^2) filled with a material with an impedance of $51Z_0$ (α_0 = 0.075; Reethof et al., 1977), randomly distributed all over the canopy volumes, with a (surface) fraction of 0.1%.

been directly included in the sound propagation equations (Van Renterghem, 2014), the current procedure avoids repeating the full simulations when making a distinction between atmospheric absorption during day and night time, as is done in this study. A homogeneous atmosphere is considered in this work. The building behind MP2 was included in the model, and related parameters can be found in Table 1.

4.4.2. ISO9613-2

Although ISO9613-2 is primarily developed to model sound propagation over flat ground, the standard allows approaching undulating terrain by the best fitted linear ground surface in between source and receiver. Source and receiver heights are then referenced to this best fitted linear profile and are called effective heights.

The ISO9613-2 simulations have been performed assuming line sources for each traffic lane, and consequently, geometrical divergence for cylindrical spreading was used. The attenuation factors in this method are essentially for point source propagation. Nevertheless, since these are referred to free field sound propagation, the equivalence between a (coherent) line source and a point source attenuation (Van Renterghem et al., 2005) can be used.

Similar to the post-processing in FDTD, atmospheric absorption was included using ISO9613-1, based on the line-of-sight distance between each traffic lane and the receiver.

The ISO9613-2 method discriminates between a source zone, a central zone and a receiver zone with relation to the ground effect. In each zone, the ground factors G are linearly averaged and weighted by the fraction they take along the ground projected path. ISO9613-2 states that ground covered by grass and soils below vegetation/trees should be modeled as porous, taking a value of G equal to 1 in the related equations (ISO 9613-2, 1996). The road surface and the cycling path get a factor G = 0 in the current case study.

The sound paths starting at the source positions in traffic lanes 1 to 3 cross the closest jersey to these lanes. For these, the ISO screening formula was used. Ground effects are disregarded then for these paths following the description in this standard (ISO 9613-2, 1996). As an illustration, the sound paths from each lane to both microphone positions are depicted in Fig. 12.

Since sound mainly propagates underneath the canopy to receiver MP2, the interaction distance between the sound path and vegetation is too limited to be considered following the vegetation module A_{other} (ISO 9613-2, 1996). The building behind MP2 was not included (see Section 6).

ISO9613-2 provides estimates in (full) octave bands (63–8000 Hz). In order to compare with the measurements that were analysed in 1/3 octave bands, the energy in each octave band was equally divided over the 3 underlying bands in an approximation. The contributions from the different lanes are energetically (and thus incoherently) summed at each receiver to calculate the total sound pressure level.

4.4.3. CNOSSOS

The concept of the CNOSSOS propagation module is quite similar to the ISO9613-2 model. The remainder of this section points at a few differences.

A similar diffraction formula for vertical screens as in ISO9613-2 is prescribed in CNOSSOS. Both screening formulae have a low evaluation complexity. The difference mainly lies in the fact that CNOSSOS uses dedicated ground interaction formulae, to be applied both at the source side and receiver side of the screen. This more extended modeling accounts for the fact that diffracted waves still interact with the ground. This is approached by including an image source and image receiver (Kephalopoulos et al., 2012).

Similarly to ISO9613-2, a ground factor G is used, linearly weighted with the fraction the different ground types take along the ground projected path. The natural soils of relevance in the current cross-section, grassland and forest floor, both belong to types B-D (Kephalopoulos et al., 2012). Although their flow resistivities are quite different, they both get the same G-value equal to 1 following this standard. The road itself and the cycling path were categorized as either ground types G or H (Kephalopoulos et al., 2012), both leading to a ground factor G equal to 0. The ground effect does not explicitly discriminate between a source zone, a central zone and a receiver zone as is done in ISO9613-2. Near the source, a factor Gs equal to 0 was used for all sound propagation paths.

The best fitted linear profile ("mean plane", see Kephalopoulos et al., 2012) is used here as well to approach the embankment. For lanes 1 to 3, the best fitted ground profile needs to be defined separately for the source and receiver side of the central reservation.

Similarly to ISO9613-2, CNOSSOS only provides estimates in full octave bands, but now limited to the band with central frequency 4 kHz. In order to compare with the measurements expressed in 1/3 octave bands, the energy in each octave band was again equally divided over the 3 underlying bands. Only formulae for homogeneous atmospheric conditions were used, given the short-distance propagation. The building behind MP2 was not included (see Section 6).

4.4.4. HARMONOISE point-to-point model (HP2P)

HP2P allows for arbitrary terrain which is approached by a succession of linear segments and diffracting edges at their interfaces. The distinction between natural terrain and (vertical) obstacles like screens/barriers and buildings is not made. Diffraction is efficiently solved by using the Deygout's approximation (Deygout, 1966). In case of diffracting sound waves, the (multiple) ground reflected contributions are accounted for. Fresnel weighting is used to include low-frequency wave effects in case of reflections and diffractions. The model has been fine-tuned by accounting for coherence loss.

The jerseys forming the middle verge are approached by vertical jumps in the ground elevation profile with a very high flow resistivity.

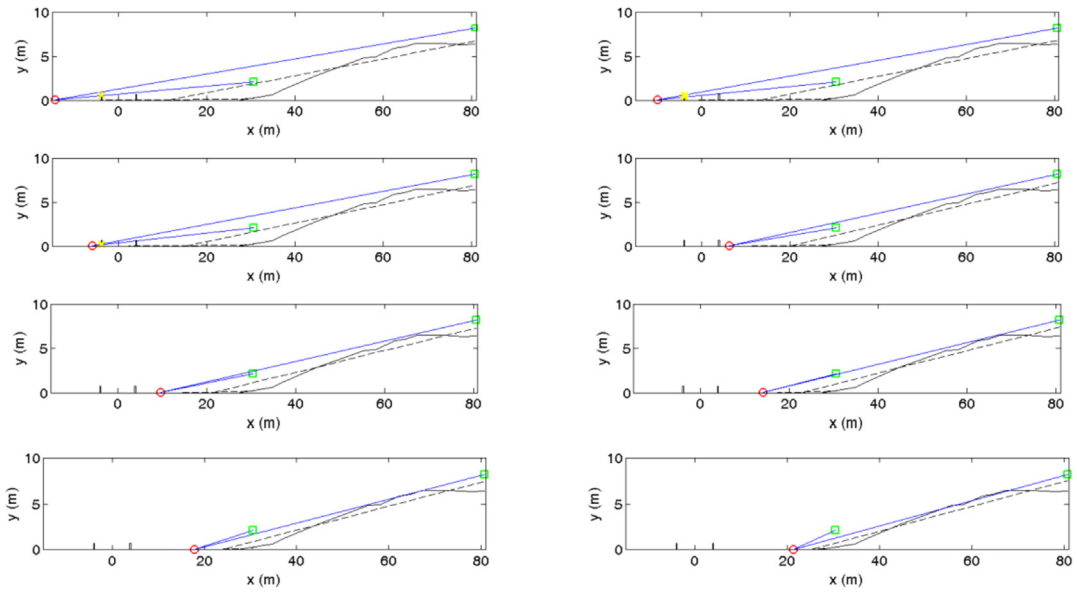

Fig. 12. Sound paths (blue lines) drawn from each traffic lane centre (red open circles) to both measurement positions (green open squares). The best fitted linear terrain profiles are indicated with the dashed lines. The intersection points with the jerseys forming the central reservation, when present, are indicated with the yellow crosses.

The model provides sound propagation predictions between a source and a receiver, expressed relative to free field sound propagation. In a next step, a similar procedure as with the other methods was applied. Cylindrical geometrical spreading and atmospheric absorption were added to calculate the total attenuation resulting from each traffic lane towards the two receiver positions. This attenuation is then subtracted from the predicted source power levels at the corresponding lane. Finally, the contributions from the different lanes are energetically summed.

Each segment takes its own ground surface impedance. New segments are defined at slope transitions, or each time an impedance transition is encountered. The one-parameter Delany and Bazley model (Delany and Bazley, 1970) was implemented in this method. Grass is modeled by an effective flow resistivity of 200 kPas/m^2, forest floor by 30 kPas/m^2. The Delany and Bazley model was shown before to be reasonably accurate to model the impedance of grassland, but larger deviations were obtained when modeling a (pine) forest floor (Attenborough et al., 2011). To make the link between the Zwikker and Kosten model (as used in FDTD) and the Delany and Bazley model, the one-parameter effective flow resistivity is approached by multiplying the flow resistivity with the porosity in a first step (Attenborough, 1985). Given the fact that this model is less accurate, some tuning of these effective flow resistivities is justified.

No meteorological refraction has been included in this validation exercise. This means that the a_{lin} and a_{log} parameters (Van Maercke and Defrance, 2007) are both set to zero, representing a homogeneous sound speed profile. Reflections from the building behind MP2 (see Section 6) were not considered.

5. Validation

The spectral level difference comparison between measurements and simulations is depicted in Fig. 13. FDTD and H2P2 show a close spectral resemblance with the measured medians at the different 1/3 octave bands. The ground effect caused by the berm is well modeled. The decrease in level difference between 800 Hz and 1.6 kHz is predicted by FDTD (which comes from scattering by the canopies, see Table 1 and sensitivity analysis in Section 6). In HP2P, this option is not available. To keep the computational cost reasonably, FDTD calculations are limited to the 1.6 kHz 1/3 octave band. H2P2 provides estimates at higher frequencies as well, although these start to deviate largely from the measurements. Note however, when looking at total A-weighted level differences (see Fig. 14), limiting calculations to the 1.6 kHz 1/3 octave band seems sufficient. The predictions by FDTD (13.3 and 13.9 dBA, for day and night conditions, respectively) are a slight underprediction of the measured medians (14.0 and 14.6 dBA, for day and night, respectively). HP2P shows a slight overprediction of the level differences (15.0 and 14.8 dBA, for day and night, respectively).

ISO9613-2 fails to predict both the soil effect and the shielding provided by the undulating terrain. The prediction is hardly any better than just accounting for geometrical divergence and atmospheric absorption (indicated as Ageo + Aatm in Figs. 13 and 14). The total A-weighted level differences between MP1 and MP2 are consequently far off, and yield 6.9 dBA (day) and 6.7 dBA (night). The CNOSSOS method predicts a significant ground dip, however, at too high sound frequencies. The transmission losses at low frequencies are too high. When looking at A-weighted level differences, CNOSSOS (10.2 dBA during the day, 9.8 dBA during the night) shows a significant improvement in accuracy relative to ISO9613-2, although the transmission loss predictions are still several decibels too low.

ISO9613-2, CNOSSOS and HP2P predict the level difference effect between day and night time conditions in the wrong direction. FDTD, in contrast, shows a similar tendency with the measurements: at night, slightly larger level differences (so more transmission losses) are found at all 1/3 octave bands, and consequently, this is also observed when looking at the total A-weighted level difference (0.6 dBA difference with FDTD). The ability to correctly predict such small effect shows the accuracy of this calculation method.

6. Sensitivity to input data

The FDTD calculations were shown to be accurate, sufficiently capturing the sound propagation physics to model the spectral level difference between MP1 and MP2 in this case of landscaping. This model is thus suited to evaluate the importance of including/neglecting geometrical aspects. Such a sensitivity study is useful for future simulation tasks where the degree of detail is lower than in this study. Five variants (cases (b)-(f), see Fig. 15) have been considered. These concern the presence of scattering vegetation elements, accounting for the ground impedance transition between grassland and forest floor on the

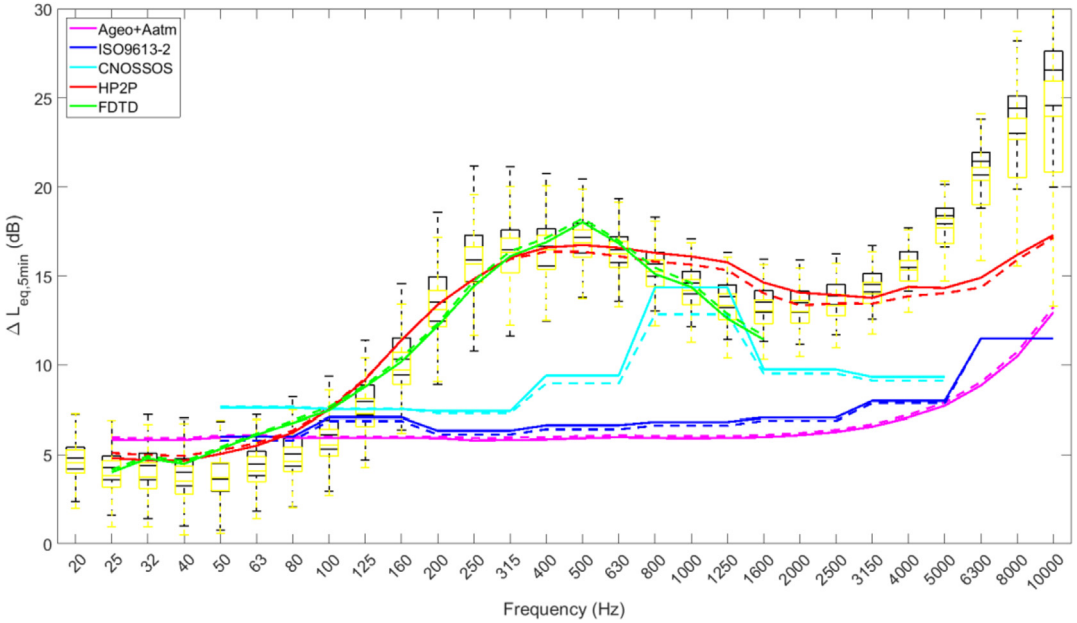

Fig. 13. Level difference spectra between MP1 and MP2, for various prediction methods. The full lines use daytime parameters, the dashed lines are for night time predictions. The simulations are plotted on top of the boxplots representing the actual measurements (yellow boxes for day time measurements, black boxes for night time measurements). Outliers (see Fig. 6) are not shown here.

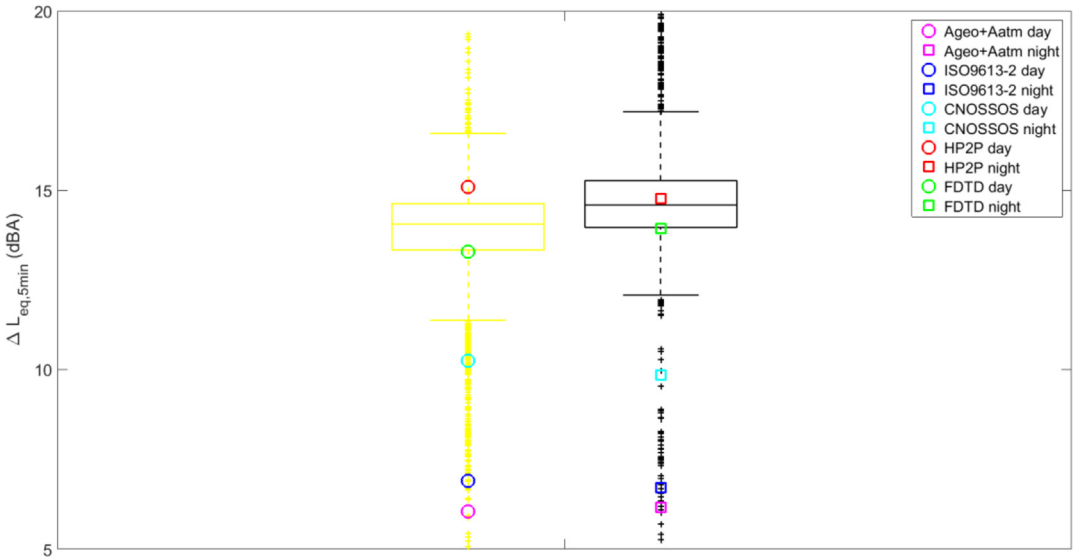

Fig. 14. See caption of Fig. 13, but now for total A-weighted level differences.

embankment, the presence of the central reservation between the two driving directions on the highway, the presence of the building behind MP2, and explicitly modeling sound propagation from all 8 traffic lanes opposed to only considering the central lane in each driving direction.

Including scattering elements to represent the trees' canopies result in a smaller level difference above 1 kHz, leading to a closer spectral resemblance with the measurements (see Fig. 16). MP2 is surrounded by canopies; downward scattering will lead to slightly increased high-frequency sound pressure levels at this location. MP1, in contrast, is expected not to be affected by vegetation.

The zone near the top of the embankment, having ground properties similar to a forest floor, contributes largely to the shielding, and consequently, to the level difference. The ground dip is much more pronounced when modeling the transition from grassland to forest floor compared to grassland applied all over the embankment. Detailed ground impedance modeling thus seems of major importance in applications of acoustical landscaping.

MP2 is positioned just at the edge of a long building parallel to the road. Including this building mainly affects the sound pressure level at MP2, and the higher sound pressure levels thus obtained at MP2 prevent overprediction of the low frequency spectral level difference. Note that in HP2P, the building was not included, which might be responsible for the small transmission loss overprediction. This effect might amount to 0.9–1.0 dBA, when using the predicted difference between case (a) and (e) with FDTD. Following this same reasoning, including this reflection in ISO9613-2 or CNOSSOS would result in a further reduction in the predicted sound pressure level differences, which was already too low to start with.

Modeling sound propagation from only the two central traffic lanes in each driving direction seems a good approach to explicitly modeling all 8 lanes. The difference between day-night propagation conditions, mainly driven by the changed (averaged) atmospheric absorption

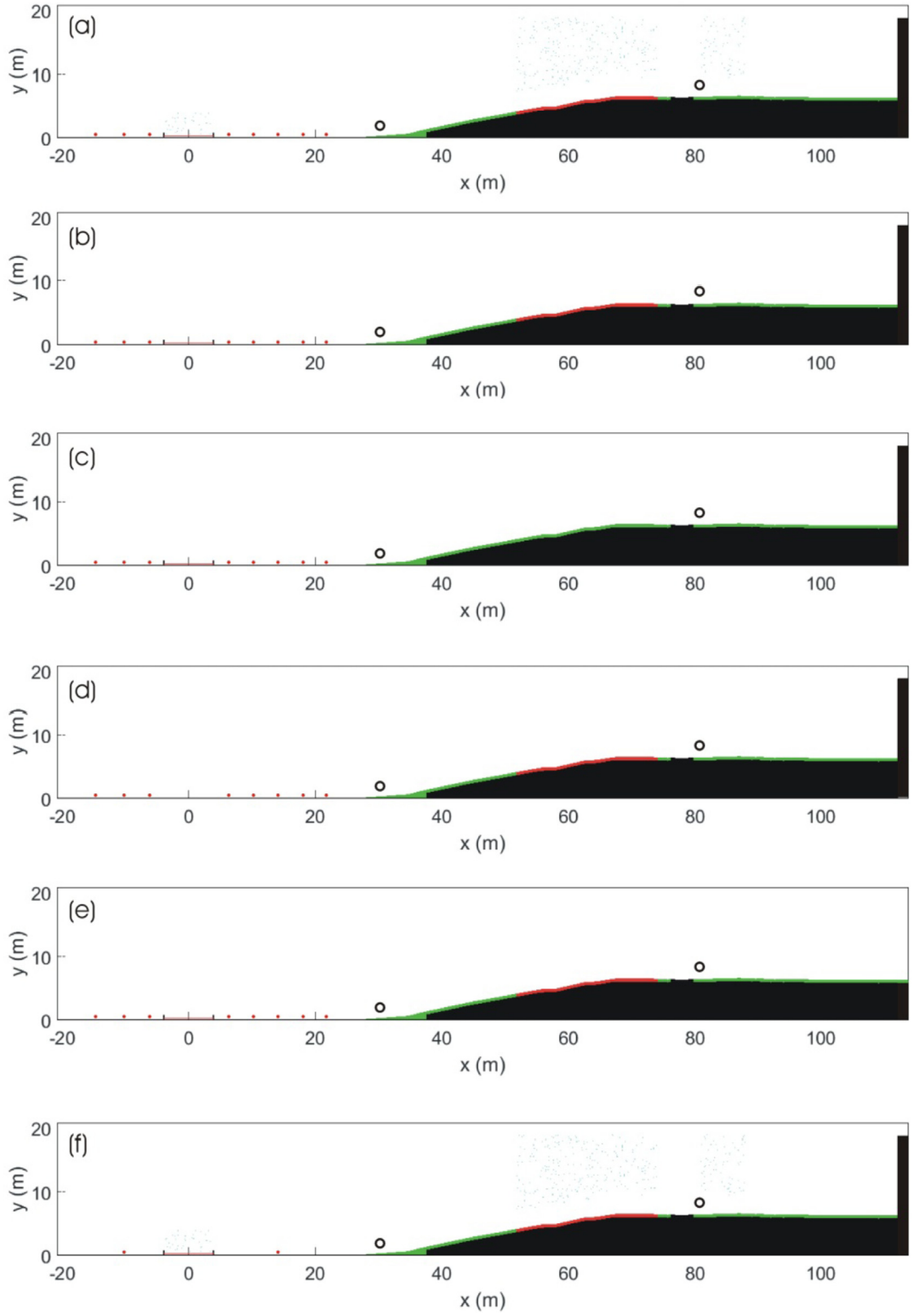

Fig. 15. Configurations considered for studying the importance of geometrical features (when using the 2D FDTD full-wave technique). In (a), the standard simulation geometry is depicted, including 8 traffic lanes, a central reservation, impedance discontinuity along the slope, vegetation (canopy), and a building facade behind MP2. In (b–e), vegetation is neglected. In (c), the ground impedance discontinuity from grassland (in green) to forest floor (in red) is neglected (only grass is considered). In (d), the central reservation is omitted. In (e), the building behind MP2 on the embankment is not considered. Case (f) is similar to (a), but only sound propagation from the middle lanes in each driving direction (but containing all sound power) was considered. The open circles indicate the locations of the microphones, the red dots the road traffic source positions (in the centers of the lanes).

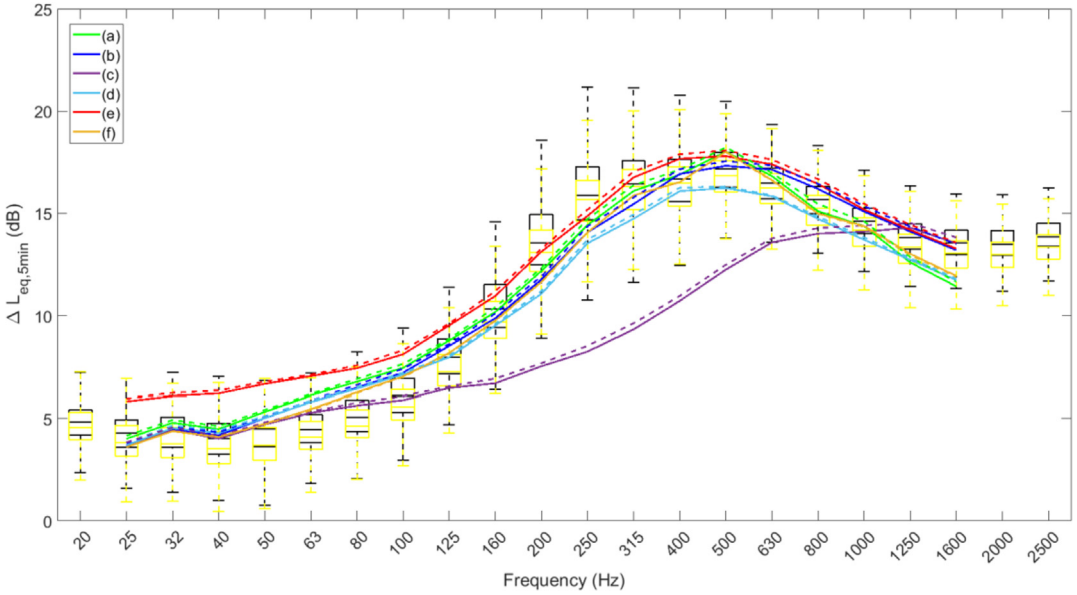

Fig. 16. Level difference spectra between MP1 and MP2, for various geometrical variants using the FDTD calculation method. Case (a) represents the simulations including full detail, cases (b)–(f) involve simplifications (see Fig. 15). The full lines are for daytime predictions, the dashed lines for night time predictions. The simulations are plotted on top of the boxplots representing the actual measurements (yellow boxes for day-time measurements, black boxes for night-time measurements). Outliers (see Fig. 6) are not shown here.

conditions and a different source power level distribution over the various lanes, amounts to a few tenths of a decibel when looking at the 1/3-octave band measurements. These effects depend on the sound frequency. For most (geometrical) variants, a similar tendency is predicted (i.e. the night time level difference is larger), but somewhat less pronounced than in the measurements. The small difference between day and night time spectral level difference cannot be made anymore when the different lanes are not modeled separately (case f, see Fig. 15) – both spectra become almost identical then (see Fig. 16).

The total A-weighted level difference predictions for the geometrical variants are summarized in Table 2. Variants (a), (b) and (e) are within 1 dBA from the median on the measurements, both during daytime and night time. In addition, the day-night level difference (i.e. 0.6 dBA) is correctly predicted by the simulations taking all details into account (case a). The most accurate prediction, when only looking at total A-weighted levels, is however case (e), which is the result of the compensation of some overpredictions at a few 1/3 octave bands by underpredictions at others. The largest deviation (among the cases modeled here) is made when grassland is considered all over the embankment (case c): a difference of 3.7 dBA relative to the measurements is then obtained.

7. Conclusions

The current sound propagation case study involves terrain shielding, mixed natural grounds, an 8-lane highway including a raised central reservation, and the presence of scattering vegetation. The sound pressure level difference measurements at two microphone positions show to be stable over time, as regards total A-weighted road traffic noise levels, but also when looking in more detail at 1/3 octave bands. Therefore, it provides a suitable but challenging sound propagation validation case. In addition, highly detailed input data was available regarding the traffic (per driving lane), measured at close distance from the cross-section under study. There was also access to detailed digital terrain elevation data.

An engineering method commonly used in noise mapping, ISO9613-2, performs poorly in predicting both spectral and total A-weighted sound pressure level differences between the microphone directly bordering the road and a second one at 80 m from the centre of the road, on the 6.3-m high embankment. The CNOSSOS method shows improved predictions and captures more of the physics relative to ISO9613-2, but still underpredicts the transmission loss with several decibels in the current case.

At the other end of the modeling spectrum, the full-wave FDTD method shows a very close spectral resemblance with the measured level difference data. Two-dimensional simulations are fully justified in such a highway configuration. Furthermore, the maximum frequency sufficiently resolved was limited to the upper frequency of the 1/3 octave band with centre frequency 1.6 kHz, and this for reasons of computational cost. However, this limitation still resulted in an accurate prediction of total A-weighted sound pressure level differences. This case study adds to other successful validation checks with

Table 2
Overview of the modeled variants with the FDTD technique, and corresponding A-weighted level differences between the assessment points 1 and 2. For comparison, the measured differences are shown as well.

	all traffic lanes	tree canopies	building behind MP2	impedance discontinuity	central reservation	ΔL (dBA) during day time.	ΔL (dBA) during night time.
measurements	x	x	x	x	x	14.0	14.6
FDTD (a)	x	x	x	x	x	13.3	13.9
FDTD (b)	x		x	x	x	13.4	14.2
FDTD (c)	x		x		x	10.3	10.8
FDTD (d)	x		x	x		12.7	13.3
FDTD (e)	x			x	x	14.2	14.9
FDTD (f)		x	x	x	x	13.0	13.5

measurements (Blumrich and Heimann, 2002; Van Renterghem and Botteldooren, 2003; Liu and Albert, 2006; Echevarria-Sanchez et al., 2016), confirming its status as reference computational model for outdoor sound propagation.

The HP2P model, accounting for terrain diffraction, shows a good spectral fit as well, but at a much lower computational cost than with FDTD. Calculation times with FDTD are in the order of hours, while HP2P only takes a few seconds. Level difference predictions between day time and night time propagation, although limited to less than 1 dB (A), could not be predicted with this method.

The sensitivity analysis to input data performed with the FDTD model further showed the importance of detailed ground impedance modeling along the embankment. It points at an additional shortcoming in engineering models like ISO9613-2 or CNOSSOS, namely their inability to account for various types of natural (porous) grounds.

Both measurements and simulations point at the important advantage of (natural) landscaping in mitigating sound propagation from a highway towards its surroundings. Not only the shape of the terrain, but also the ground properties should be controlled for (Attenborough et al., 2016). This type of noise reducing measure should therefore be promoted in future highly noise-exposed traffic environments on condition that the necessary space is available.

Data and software availability

The FDTD sound propagation model is a research code written in C++, developed during the past decades at the Department of Information Technology at Ghent University. The main parts of this code were written by the authors of the current paper. Neither the source code nor executables are publicly available.

The HP2P sound propagation calculations were performed with the publicly available PointToPoint.dll (v. 2.0120, D. Van Maercke), developed within the framework of the European Commission's projects HARMONOISE (Framework Program 5, FP5) and IMAGINE (FP6). This library has been called from a Python script to automate the simulations.

The ISO9613-2 and CNOSSOS propagation models are own implementations in Matlab (v2017a, MathWorks company), partly relying on a freely available library containing geometrical functions namely geom2d (v 1.24, D. Legland, Matlab File Exchange platform). Splitting up the terrain in linear segments, which was a necessary input to the HP2P model, was based on the dpsimplify.m function (v 1.4, W. Schwanghart, Matlab File Exchange platform).

All other pre- and post-processing were performed with Matlab.

The measurement data is available (upon request) for similar model validation exercises.

Author contributions

T.V. and D.B. designed the research. T.V. performed the measurements and data processing, and conducted all simulations. T.V. wrote the paper and did the analyses, D.B. did the proofreading.

Declarations of interest

None.

Acknowledgments

The authors are grateful to the city of Antwerp for funding the measurement campaign on which the current validation study is based.

References

Arenas, J., 2008. Potential problems with environmental sound barriers when used in mitigating surface transportation noise. Sci. Total Environ. 405, 173–179.
Attenborough, K., 1985. Acoustical impedance models for outdoor ground surfaces. J. Sound Vib. 99, 521–544.
Attenborough, K., Li, K., Horoshenkov, K., 2007. Predicting Outdoor Sound. Taylor and Francis, London and New York.
Attenborough, K., Bashir, I., Taherzadeh, S., 2011. Outdoor ground impedance models. J. Acoust. Soc. Am. 129, 2806–2819.
Attenborough, K., Bashir, I., Taherzadeh, S., 2016. Exploiting ground effects for surface transport noise abatement. Noise Mapp. J. 3, 1–25.
Berglund, B., Lindvall, T., Schwela, D., 1999. Guidelines for Community Noise. World Health Organization, Geneva.
Blumrich, R., Heimann, D., 2002. A linearized Eulerian sound propagation model for studies of complex meteorological effects. J. Acoust. Soc. Am. 112, 446–455.
Botteldooren, D., Dekoninck, L., Gillis, D., 2011. The influence of traffic noise on appreciation of the living quality of a neighborhood. Int. J. Environ. Res. Publ. Health 8, 777–798.
Busch, T., Hodgson, M., Wakefield, C., 2003. Scale-model study of the effectiveness of highway noise barriers. J. Acoust. Soc. Am. 114, 1947–1954.
Cox, T., D'Antonio, P., 2004. Acoustic Absorbers and Diffusers: Theory, Design and Application. Taylor and Francis, London and New York.
Cramond, A., Don, C., 1987. Effect of moisture content on soil impedance. J. Acoust. Soc. Am. 82, 293–301.
De Jong, R., Stusnick, E., 1976. Scale model studies of the effect of wind on acoustic barrier performance. Noise Contr. Eng. 6, 101–109.
Defrance, J., Salomons, E., Noordhoek, I., Heimann, D., Plovsing, B., Watts, G., Jonasson, H., Zhang, X., Premat, E., Schmich, I., Aballea, F., Baulac, M., de Roo, F., 2007. Outdoor sound propagation reference model developed in the European Harmonoise project. Acta Acust. united Ac 93, 213–227.
Delany, M., Bazley, E., 1970. Acoustical properties of fibrous absorbent materials. Appl. Acoust. 3, 105–116.
Deygout, J., 1966. Multiple knife-edge diffraction by microwaves. IEEE Trans. Antenn. Propag. 14, 480–489.
Dutilleux, G., Defrance, J., Ecotière, D., Gauvreau, B., Bérengier, M., Besnard, F., Le Duc, E., 2010. NMPB-Routes-2008: the revision of the French method for road traffic noise prediction. Acta Acust. united Ac 96, 452–462.
Echevarria-Sanchez, G., Van Renterghem, T., Thomas, P., Botteldooren, D., 2016. The effect of street canyon design on traffic noise exposure along roads. Build. Environ. 97, 96–110.
Embleton, T., 1996. Tutorial on sound propagation outdoors. J. Acoust. Soc. Am. 100, 31–48.
Fritschi, L., Brown, L., Kim, R., Schwela, D., Kephalopoulos, S., 2011. Burden of Disease from Environmental Noise—quantification of Healthy Life Years Lost in Europe. WHO regional office for Europe.
Guillaume, G., Faure, O., Gauvreau, B., Junker, F., Bérengier, M., L'Hermite, P., 2015. Estimation of impedance model input parameters from in situ measurements: principles and applications. Appl. Acoust. 95, 27–36.
Hong, J., Jeon, J., 2014. The effects of audio-visual factors on perceptions of environmental noise barrier performance. Landscape urban plan 125, 28–37.
ISO 9613-1, 1996. Acoustics – Attenuation of Sound during Propagation Outdoors – Part 1. International Organisation for Standardisation, Geneva, Switzerland.
ISO 9613-2, 1996. Acoustics – Attenuation of Sound during Propagation Outdoors – Part 2. International Organisation for Standardisation, Geneva, Switzerland.
Jonasson, H., 1972. Sound reduction by barriers on the ground. J. Sound Vib. 22, 113–126.
Jonasson, H., 2007. Acoustical source modelling of road vehicles. Acta Acust. united Ac 93, 173–184.
Kaplan, R., Kaplan, S., 1989. The Experience of Nature: a Psychological Perspective. Cambridge University Press, New York.
Kephalopoulos, S., Paviotti, M., Anfosso-Lédée, F., 2012. Common Noise Assessment Methods in Europe (CNOSSOS-EU). Publications office of the European Union.
Keyel, A., Reed, S., McKenna, M., Wittemyer, G., 2017. Modeling anthropogenic noise propagation using the Sound Mapping Tools ArcGIS toolbox. Environ. Model. Software 97, 56–60.
Kotzen, B., English, C., 2009. Environmental Noise Barriers – a Guide to Their Acoustic and Visual Design, second ed. Taylor and Francis, London.
Licitra, G., 2013. Noise Mapping in the EU: Models and Procedures. Taylor and Francis group (CRC press), Boca Raton-London-New York.
Liu, L., Albert, D., 2006. Acoustic pulse propagation near a right-angle wall. J. Acoust. Soc. Am. 119, 2073–2083.
Maffei, L., Masullo, M., Aletta, F., Di Gabriele, M., 2013. The influence of visual characteristics of barriers on railway noise perception. Sci. Total Environ. 445–446, 41–47.
Morgan, S., Kay, D., Bodapati, S., 2001. Study of noise barrier life-cycle costing. J. Transport. Eng. 127, 230–236.
Nilsson, M., Andéhn, M., Leśna, P., 2008. Evaluating roadside noise barriers using an annoyance-reduction criterion. J. Acoust. Soc. Am. 124, 3561–3567.
Nilsson, M., Bengtsson, J., Klaeboe, R., 2014. Environmental Methods for Transport Noise Reduction. Taylor and Francis, CRC Press, Boca Raton, London, New York.
Nugent, C., Blanes, N., Fons, J., Sáinz de la Maza, M., José Ramos, M., Domingues, F., van Beek, A., Houthuijs, D., 2014. Noise in Europe 2014. European Environment Agency, Report 10/2014. Publication Office of the European Union, Luxembourg.
Oltean-Dumbrava, C., Miah, A., 2016. Assessment and relative sustainability of common types of roadside noise barriers. J. Clean. Prod. 135, 919–931.
Ramer, U., 1972. An iterative procedure for the polygonal approximation of plane curves. Comput Vision Graph 1, 244–256.
Reethof, G., Frank, L., McDaniel, O., 1977. Sound absorption characteristics of treebark and forest floor. In: Proceedings of the Conference on Metropolitan Physical

Environment, USDA Forest Service General Technical Report NE-2.
Salomons, E., 1999. Reduction of the performance of a noise screen due to screen-induced wind-speed gradients. Numerical computations and wind tunnel experiments. J. Acoust. Soc. Am. 105, 2287–2293.
Sandberg, U., Ejsmont, J., 2002. Tyre/road Noise Reference Book. Informex, Kisa.
Van Maercke, D., Defrance, J., 2007. Development of an analytical model for outdoor sound propagation within the Harmonoise project. Acta Acta Acust. united Ac 93, 201–212.
Van Renterghem, T., 2014. Efficient outdoor sound propagation modeling with the finite-difference time-domain (FDTD) method: a review. Int. J. Aeroacoustics 13, 385–404.
Van Renterghem, T., 2018. Towards explaining the positive effect of vegetation on the perception of environmental noise. Urban For. Urban Green (in press). https://doi.org/10.1016/j.ufug.2018.03.007.
Van Renterghem, T., Botteldooren, D., 2003. Numerical simulation of the effect of trees on downwind noise barrier performance. Acta Acust. united Ac 89, 764–778.
Van Renterghem, T., Botteldooren, D., 2012. On the choice between walls and berms for road traffic noise shielding including wind effects. Landsc. Urban Plann. 105, 199–210.
Van Renterghem, T., Salomons, E., Botteldooren, D., 2005. Efficient FDTD-PE model for sound propagation in situations with complex obstacles and wind profiles. Acta Acust. united Ac 91, 671–679.
Zwikker, C., Kosten, C., 1949. Sound Absorbing Materials. Elsevier, New York.